Operation and Design Principles of Biological/Artificial Molecular Machines

Department of Life and Coordination-Complex Molecular Science
Division of Biomolecular Functions

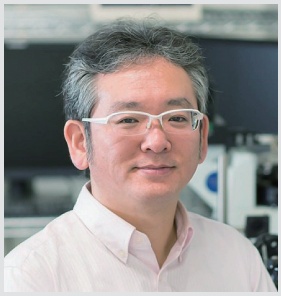

IINO, Ryota
Professor
[iino@ims.ac.jp]

Education
1995 B.E. Kyoto University
1997 M.E. Kyoto University
2003 Ph.D. Nagoya University

Professional Employment
2000 Research Associate, Japan Science and Technology Corporation
2002 Research Associate, Japan Science and Technology Agency
2005 Specially-Appointed Assistant Professor, Osaka University
2006 Assistant Professor, Osaka University
2011 Lecturer, The University of Tokyo
2013 Associate Professor, The University of Tokyo
2014 Professor, Institute for Molecular Science
Professor, Okazaki Institute for Integrative Bioscience (–2018)
Professor, The Graduate University for Advanced Studies

Award
2012 Emerging Investigator. Lab on a Chip., The Royal Society of Chemistry, U.K.

Member
Assistant Professor
OTOMO, Akihiro
HARASHIMA, Takanori
Visiting Scientist
MEKSERIWATTANA, Wid*
BOUISSET, Tom*
Technical Support Staff
YAMAMOTO, Mayuko
Secretary
NOMURA, Junko
KAWAGUCHI, Ritsuko

Keywords Molecular Motors, Single-Molecule Biophysics, Protein Engineering

Life is supported by protein molecular machines which show better performance than man-made machines. One representative of the protein molecular machines is molecular motors (Figure 1). Molecular motors show autonomous unidirectional motions using the energy of chemical reaction. We unveil operational principles of molecular motors with advanced single-molecule analysis. In addition, with protein engineering, we create non-natural/hybrid molecular motors to understand their design principles. Furthermore, we create DNA/RNA-based artificial molecular motors and motor systems that mimic and outperform biological ones.

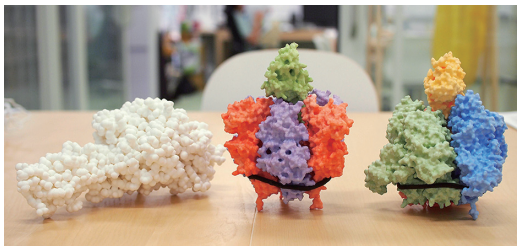

Figure 1. Protein molecular machines. (Left) A linear molecular motor chitinase A. (Center and Right) Rotary molecular motors F_1-ATPase and V_1-ATPase, respectively.

Selected Publications

- A. Otomo, L. G. Hui Zhu, Y. Okuni, M. Yamamoto and R. Iino, "ATP Synthesis of *Enterococcus hirae* V-ATPase Driven by Sodium Motive Force," *J. Biol. Chem.* **301**, 108422 (2025).
- K. Suzuki, Y. Goto, A. Otomo, K. Shimizu, S. Abe, K. Moriyama, S. Yasuda, Y. Hashimoto, J. Kurushima, S. Mikuriya, F. L. Imai, N. Adachi, M. Kawasaki, Y. Sato, S. Ogasawara, S. Iwata, T. Senda, M. Ikeguchi, H. Tomita, R. Iino, T. Moriya and T. Murata, "Na^+-V-ATPase Inhibitor Curbs VRE Growth and Unveils Na^+ Pathway Structure," *Nat. Struct. Mol. Biol.* **32**, 450–458 (2025).
- T. Harashima, A. Otomo and R. Iino, "Rational Engineering of DNA-Nanoparticle Motor with High Speed and Processivity Comparable to Motor Proteins," *Nat. Commun.* **16**, 729 (2025).
- A. Otomo, J. Wiemann, S. Bhattacharyya, M. Yamamoto, Y. Yu and R. Iino, "Visualizing Single V-ATPase Rotation Using Janus Nanoparticles," *Nano Lett.* **24**, 15638–15644 (2024).
- T. Kosugi, T. Iida, M. Tanabe, R. Iino and N. Koga, "Design of Allosteric Sites into Rotary Motor V_1-ATPase by Restoring Lost Function of Pseudo-Active Sites," *Nat. Chem.* **15**, 1591–1598 (2023).
- A. Otomo, T. Iida, Y. Okuni, H. Ueno, T. Murata and R. Iino, "Direct Observation of Stepping Rotation of V-ATPase Reveals Rigid Component in Coupling between V_o and V_1 Motors," *Proc. Natl. Acad. Sci. U. S. A.* **119**, e2210204119 (2022).
- A. Nakamura, N. Kobayashi, N. Koga and R. Iino, "Positive Charge Introduction on the Surface of Thermostabilized PET Hydrolase Facilitates PET Binding and Degradation," *ACS Catal.* **11**, 8550–8564 (2021).
- R. Iino, K. Kinbara and Z. Bryant, "Introduction: Molecular Motors," *Chem. Rev.* **120**, 1–4 (2020).
- J. Ando, A. Nakamura, M. Yamamoto, C. Song, K. Murata and R. Iino, "Multicolor High-Speed Tracking of Single Biomolecules with Silver, Gold, Silver-Gold Alloy Nanoparticles," *ACS Photonics* **6**, 2870–2883 (2019).
- A. Nakamura, K. Okazaki, T. Furuta, M. Sakurai and R. Iino, "Processive Chitinase is Brownian Monorail Operated by Fast Catalysis after Peeling Rail from Crystalline Chitin," *Nat. Commun.* **9**, 3814 (2018).

1. ATP Synthesis of *Enterococcus hirae* V-ATPase Driven by Sodium Motive Force[1)]

V-ATPases generally function as ion pumps driven by ATP hydrolysis in the cell, but their capability of ATP synthesis remains largely unexplored. Here we show ATP synthesis of Na^+-transporting *Enterococcus hirae* V-ATPase (EhV_oV_1) driven by the electrochemical potential gradient of Na^+ across the membrane (sodium motive force, *smf*). We reconstituted EhV_oV_1 into liposome and performed a luciferin/luciferase-based assay to analyze ATP synthesis quantitatively. Our result demonstrates that EhV_oV_1 synthesizes ATP with a rate of 4.7 s^{-1} under high *smf* (269.3 mV). The Michaelis constants for ADP (21 μM) and inorganic phosphate (2.1 mM) in ATP synthesis reaction were comparable to those for ATP synthases, suggesting similar substrate affinities among rotary ATPases regardless of their physiological functions. Both components of *smf*, Na^+ concentration gradient across the membrane (ΔpNa) and membrane potential (Δψ), contributed to ATP synthesis. At the equilibrium points where *smf* and Gibbs free energy of ATP synthesis are balanced, EhV_oV_1 showed reversible reactions between ATP synthesis and hydrolysis (Figure 2). The obtained Na^+/ATP ratio (3.2 ± 0.4) closely matched the value expected from the structural symmetry ratio between EhV_o and EhV_1 (10/3 = 3.3), indicating tight coupling between ATP synthesis/hydrolysis and Na^+ transport. These results reveal the inherent functional reversibility of EhV_oV_1. We propose that the physiological function of EhV_oV_1 *in vivo* is determined by relatively small *smf* against large Gibbs free energy of ATP synthesis.

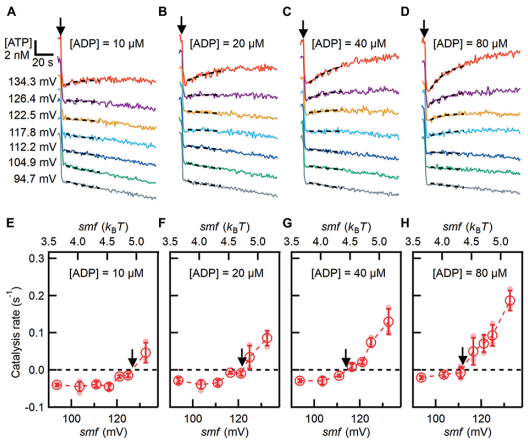

Figure 2. Determination of equilibrium points between ATP synthesis and hydrolysis. *A–D*, time courses of ATP synthesis and hydrolysis at different *smf* (93.5–132.6 mV). Reaction was initiated by adding proteoliposome as indicated by black arrow. The black dashed lines represent the fitting with a single exponential function for Δt = 35 s after the addition of PL. *E–H*, *smf* dependence of ATP synthesis and hydrolysis rates. Black arrows indicate equilibrium points obtained by linear fitting between two data points across the catalysis rate of zero. The reaction solution contains 25 nM ATP, 9.95 mM Pi, and ADP at 10 μM (*A* and *E*), 20 μM (*B* and *F*), 40 μM (*C* and *G*), and 80 μM (*D* and *H*), respectively.

2. Na^+-V-ATPase Inhibitor Curbs VRE Growth and Unveils Na^+ Pathway Structure[2)]

Vancomycin-resistant *Enterococcus faecium* (VRE) is a major cause of nosocomial infections, particularly endocarditis and sepsis. With the diminishing effectiveness of antibiotics against VRE, new antimicrobial agents are urgently needed. Our previous research demonstrated the crucial role of Na^+-transporting V-ATPase in *Enterococcus hirae* (EhV_oV_1) for growth under alkaline conditions. In this study, we identified a compound, V-161, from 70,600 compounds, which markedly inhibits EhV_oV_1 activity (Figure 3). V-161 not only inhibits VRE growth in alkaline conditions but also significantly suppresses VRE colonization in the mouse small intestine. Furthermore, we unveiled the high-resolution structure of the membrane V_o part due to V-161 binding. V-161 binds to the interface of the c-ring and a-subunit, constituting the Na^+ transport pathway in the membrane, thereby halting its rotation. This structural insight presents potential avenues for developing therapeutic agents for VRE treatment and elucidates the Na^+ transport pathway and mechanism.

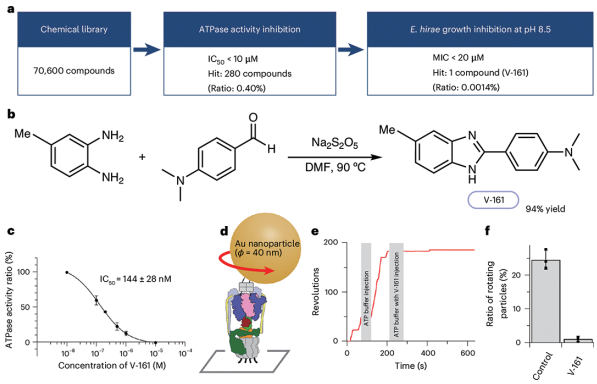

Figure 3. Schematic of screening process for EhV_oV_1 inhibitors. **b**, Chemical synthesis route of V-161. **c**, Inhibition of ATPase activity of EhV_oV_1 by V-161. Results are shown as mean ± s.e.m., derived from three separate experiments. **d**, Schematic of single-molecule rotation assay for EhV_oV_1. **e**, Rotation time course. After an initial 1 min of rotation recording, a buffer with 10 μM ATP was injected (indicated by the first gray square). After another several minutes of recording, a buffer containing both 2 μM V-161 and 10 μM ATP was injected (indicated by the second gray square). The recording speed was set to 50 frames per second. **f**, Ratio of rotating particles relative to the total particles attached to the glass surface. Results are shown as mean ± s.d., derived from three separate experiments.

References

1) A. Otomo, L. G. Hui Zhu, Y. Okuni, M. Yamamoto and R. Iino, *J. Biol. Chem.* **301**, 108422 (2025).
2) K. Suzuki, Y. Goto, A. Otomo, K. Shimizu, S. Abe, K. Moriyama, S. Yasuda, Y. Hashimoto, J. Kurushima, S. Mikuriya, F. L. Imai, N. Adachi, M. Kawasaki, Y. Sato, S. Ogasawara, S. Iwata, T. Senda, M. Ikeguchi, H. Tomita, R. Iino, T. Moriya and T. Murata, *Nat. Struct. Mol. Biol.* **32**, 450–458 (2025).

* IMS International Internship Program